Trop. J. of Eng., Sci. and Techn. 2022. 1(1):14-50
@Tropical Journal of Engineering, Science and Technology.

Groundwater Potential Mapping Using Geophysical Data and Entropy Method in a Typical Basement Complex Environment, Southwestern Nigeria

Akinlalu, Ayokunle Adewale, Adebayo, Olanrewaju Stephen, Afolabi, Daniel Oluwafunmilade

Department of Applied Geophysics, Federal University of Technology, Akure.
Corresponding Author;danielafolabi31@gmail.com; afolabido@futa.edu.ng;

Abstract

The study applied an objective method of weight assignment involving the entropy method to assign weights to groundwater conditioning factors in order of their relative importance to groundwater potential in a typical basement complex environment of southwestern, Nigeria. The groundwater conditioning factors involving aquifer resistivity, overburden thickness, coefficient of reflection, co-efficient of anisotropy and bedrock topography are geoelectric parameters obtained from the electrical resistivity data. Weights assignment using the entropy method shows that the groundwater conditioning factors in order of their importance are aquifer resistivity, overburden thickness, coefficient of reflection, coefficient of anisotropy and bedrock topography. Maps of the weighted conditioning factors were integrated in GIS environment to produce the groundwater potential map of the study area. The groundwater potential map was subsequently subjected to concentration area (C–A) fractal modeling to classify the maps into five classes into background; low; moderate; high and very high in a data driven way. The background anomaly indicated areas of no groundwater potential. The classified groundwater potential map showed that areas of background and low groundwater potential are located majorly in the western flank of the study area coinciding spatially with the occurrence of charnockite. Furthermore, areas of moderate to very high groundwater potential are majorly located in the northern flank of the study area, extending through the central flank to the eastern flank of the study area, coinciding spatially majorly with granite in the study area. The study showed that granite in the study area is the most promising in terms of groundwater potential because it favors the performance of the groundwater conditioning index used in this study. The validation of the groundwater potential map generated with the productive water wells in the study area shows 75% agreement which showed that the model used in this study is a workable model for groundwater potential mapping. It can further guide water resource experts on groundwater mapping and management in the study area and other similar geologic environments in the world.

Keywords: Groundwater conditioning factors; entropy model; geoelectric parameters; groundwater potential mapping; concentration area (C–A) fractal model.

Cartographie du potentiel des eaux souterraines à l'aide de données géophysiques et de la méthode d'entropie dans un environnement complexe de sous-sol typique, sud-ouest du Nigeria

Résumé

L'étude a appliqué une méthode objective d'attribution de poids impliquant la méthode d'entropie pour attribuer des poids aux facteurs de conditionnement des eaux souterraines dans l'ordre de leur importance relative pour le potentiel des eaux souterraines dans un environnement complexe de sous-sol typique du sud-ouest du Nigeria. Les facteurs de conditionnement des eaux souterraines impliquant la résistivité de l'aquifère, l'épaisseur du mort-terrain, le coefficient de réflexion, le coefficient d'anisotropie et la topographie du substrat rocheux sont des paramètres géoélectriques obtenus à partir des données de résistivité électrique. L'attribution des pondérations à l'aide de la méthode d'entropie montre que les facteurs de conditionnement des eaux souterraines par ordre d'importance sont la résistivité de l'aquifère, l'épaisseur du mort-terrain, le coefficient de réflexion, le coefficient d'anisotropie et la topographie du substrat rocheux. Des cartes des facteurs de conditionnement pondérés ont été intégrées dans l'environnement SIG pour produire la carte du potentiel des eaux souterraines de la zone d'étude. La carte du potentiel des eaux souterraines a ensuite été soumise à une modélisation fractale de la zone de concentration (C – A) pour classer les cartes en cinq classes en arrière-plan ; bas; modéré; élevé et très élevé d'une manière axée sur les données. L'anomalie de fond indiquait des zones sans potentiel d'eaux souterraines. La carte classée du potentiel des eaux souterraines a montré que les zones de fond et de faible potentiel des eaux souterraines sont situées principalement dans le flanc ouest de la zone d'étude coïncidant spatialement avec la présence de charnockite. De plus, les zones à potentiel hydrique souterrain modéré à très élevé sont principalement situées sur le flanc nord de la zone d'étude, s'étendant du flanc central jusqu'au flanc est de la zone d'étude, coïncidant spatialement avec le granite dans la zone d'étude. L'étude a montré que le granite de la zone d'étude est le plus prometteur en termes de potentiel d'eau souterraine car il favorise la performance de l'indice de conditionnement des eaux souterraines utilisé dans cette étude. La validation de la carte du potentiel des eaux souterraines générée avec les puits d'eau productifs dans la zone d'étude montre un accord de 75 %, ce qui montre que le modèle utilisé dans cette étude est un modèle exploitable pour la cartographie du potentiel des eaux souterraines. Il peut en outre guider les experts en ressources en eau sur la cartographie et la gestion des eaux souterraines dans la zone d'étude et d'autres environnements géologiques similaires dans le monde.

Mots-clés : Facteurs de conditionnement des eaux souterraines; modèle d'entropie ; paramètres géoélectriques ; cartographie du potentiel des eaux souterraines ; modèle fractal de zone de concentration (C – A).

رسم خرئط إمكانات المياه الجوفية باستخدام البيانات الجيوفيزيائية وطريقة الانتروبيا في بيئة معقدة في الطابق السفلى النموذجي جنوب غرب نيجيريا

نبذة مختصرة

طبقت الدراسة طريقة موضوعية لتخصيص الوزن تتضمن طريقة الانتروبي التعيين أوزان لعوامل تكييف المياه الجوفية بالترتيب من حيث أهميتها النسبية لإمكانات المياه الجوفية في بيئة معقد قاعدي نموذجي في جنوب غرب نيجيريا. إن عوامل تكييف المياه الجوفية التي تتضمن مقاومة الخزان الجوفي، وسمك الطبقة السطحية، ومعامل الانعكاس، ومعامل تباين الخواص وطبو غرافيا القاعدة هي معلما تجي وكهر بائية تم الحصول عليها من بيانات المقاومة الكهربائية. يوضحت خصيص الأوزان باستخدام طريقة الانتروبيا أن عوامل تكييف المياه الجوفية بالترتيب من حيث أهميتها هي مقاومة الخزان الجوفي، وسمك الطبقة السطحية، ومعامل الانعكاس، ومعامل تباين الخواص، وطب وغرافيا القاعدة. تم دمج خرائط عوامل التكييف الموزونة في بيئة نظم المعلومات الجغرافية لإنتاج خريطة احتمالية المياه الجوفية لمنطقة الدراسة. تم إخضاع خريطة احتمالية المياه الجوفية لاحقًا لنمذجة منطقة التركيز (C-A) لتصنيف الخرائط إلى خمس فئات في الخلفية؛ قليل؛ معتدل؛ عالية وعالية جدًا بطريقة تعتمد على البيانات. يشير الشذوذ في الخلفية إلى مناطق لا توجد فيها إمكانية للمياه الجوفية. أظهر تخريطة إمكانات المياه الجوفية المصنفة أن مناطق الخلفية وانخفاض إمكانيات المياه الجوفية تقع بشكل رئيسي في الجانب الغربي من منطقة الدراسة متزامنة مكانيًا معوجود الكارنوكيت. علاوة على ذلك، فإن المناطق ذات الإمكانات المتوسطة إلى العالية جدًا للمياه الجوفية تقع بشكل رئيسي في الجهة الشمالية من منطقة الدراسة، وتمتد من خلالا لجناح المركزي إلى الجانب الشرقي من منطقة الدراسة، متزامنة بشكل مكاني مع الجرانيت في منطقة الدراسة. أوضحت الدراسة أن الجرانيت في منطقة الدراسة هو الأكثر واعدة من حيث إمكانات المياه الجوفية لأنه يفضل أداء مؤشر تكييف المياه الجوفية المستخدم في هذه الدراسة. يُظهر التحقق من صحة خريطة احتمالية المياه الجوفية الناتجة عن آبار المياه المنتجة في منطقة الدراسة اتفاقًا بنسبة (75%) مما أظهر أن النموذج المستخدم في هذه الدراسة هو نموذج عملي لرسم خرائط إمكانات المياه الجوفية. يمكن أن يوجه خبراء الموارد المائية أيضًا حول رسم خرائط المياه الجوفية وإدارتها في منطقة الدراسة والبيئات الجيولوجية المماثلة الأخرى في العالم.

الكلمات المفتاحية: عوامل تكييف المياها لجوفية. نموذج الانتروبيا معلمات جيوكهر بائية رسم الخرائط المحتملة للمياه الجوفية؛ منطقة التركيز (C – A) نموذج كسوري.

Introduction

Water is life and its importance to human existence on planet earth cannot be overemphasized. The demand for water for human consumption and other needs is ever increasing especially in areas experiencing rapid population growth and physical development. High percentage of water users in the world rely substantially on groundwater (Reilly *et al.*, 2008). Groundwater contributes substantially to meet the water needs for most domestic, municipal and industrial purposes worldwide, due to its availability in almost all parts of the world. In addition, and most importantly, very minor water treatment is often required to make it potable. Although water is a renewable resource, yet its supply in suitable quality is steadily decreasing due to poor groundwater management and effect of poor waste water management, especially in developing countries like Nigeria. Moreover, the demand of this resource has increased significantly throughout the world due to population growth, socio-economic development, technological and

climatic changes (Olayinka *et al.,* 1999; Alcamo, 2007).

The problems arising from groundwater occurrence, abstraction and contamination abounds in different geologic settings around the world (Akinlalu *et al.,* 2017; Akinlalu and Afolabi, 2018; Adesola *et al.,* 2021). Each geologic setting has its peculiar problem regarding groundwater. In the sedimentary terrains, groundwater problems arise majorly from saline contamination and the ease of contamination of effluent into groundwater systems due to the porous nature of the lithologies present (Akinlalu and Afolabi, 2018). In the basement complex geological environment which is made up of crystalline rocks, groundwater problems arise majorly from the potential of locating groundwater for usage (Adepelumi *et al.,* 2006; Bayode *et al.,* 2007; Adiat *et al.,* 2018). This is majorly because the rocks are not very porous and permeable. Hence, groundwater occurrences are associated with pocket of spaces where the rocks are fractured, or where the presence of fissures, rock contacts or geologic structures such as faults, joints etc. permits the migration of groundwater. Locating these pockets of spaces presents an even greater problem to groundwater developers as the structures accommodating groundwater are several meters below the ground surface, making visual observation difficult in groundwater exploration (Olayinka and Olorunfemi, 1992; Omosuyi and Oyemola, 2012; Akinlalu *et al.,* 2017).

This makes geophysical method an ideal method in groundwater exploration, due to its ability to delineate and map structures that are probable hosts to groundwater. Various geophysical methods such as magnetic, gravity, seismic refraction, electromagnetic and electrical resistivity methods have been applied successfully in the exploration of groundwater (Olayinka and Olorunfemi, 1992; Omosuyi and Oyemola, 2012; Akinlalu *et al.,* 2017; Adiat *et al.,* 2018; Adesola *et al.,* 2021). Geophysical methods are suitable in the exploration of groundwater because of the ability to probe deep into the subsurface to locate geologic structures harboring groundwater. Also, they are able to map the geometry of the bedrock. However, the commonest geophysical method employed in groundwater exploration is the electrical resistivity method (Olorunfemi and Okhue, 1992; Omosuyi *et al.,* 2003; Akinlalu *et al.,* 2017). This is due to its ability to probe deep into the subsurface and its unique potential of differentiating lithologic units. Therefore, the urge to sustain groundwater need by people has strengthened the application of appropriate geophysical and/or hydrogeologic search (Olayinka *et al*., 1999; Olorunfemi *et al*., 1999; Lashkaripour, 2003; Batayneh, 2010; Omosuyi, 2010; Anudu *et al*., 2011) to locate areas of high and reliable groundwater prospect or characterize seasonal changes in the near surface aquifer (Webb *et al*., 2011).

Nowadays, groundwater exploration on a large scale involves groundwater potential mapping which is a targeted program geared at combining and integrating conditioning factors that favor groundwater accumulation and storage. The integration of conditioning factors like lithologies, topography, lineament density, coefficient of anisotropy, rainfall intensity, drainage, aquifer resistivity, overburden thickness, aquifer thickness etc. are used in creating models of groundwater potential (Adiat, *et al.,*2013; Akinlalu *et al.,* 2017; Adiat *et al.,* 2018; Akinlalu *et al.,* 2021). The knowledge–and data–driven models have been used extensively in groundwater

potential mapping in various geologic settings of the world.

For the Knowledge–driven models, geoscientists' expert judgment is applied to weight evidential features. Boolean logic, index overlay, evidential belief functions, fuzzy logic, analytical hierarchal process (AHP), fuzzy AHP, Stepwise Weight Assessment Ratio Analysis (SWARA) are some of the widely employed knowledge–driven models (Moon, 1990; Chung and Moon, 1990; An *et al*., 1991; Bonham-Carter, 1994; Nykänen and Salmirinne, 2007; Carranza, 2008; Akinlalu *et al.,* 2017; Forson *et al*., 2020; Sanusi and Amigun, 2020; Akinlalu *et al*., 2021). The success of the knowledge–driven model has been reported by several workers in groundwater potential mapping (Adiat *et al.,* 2012; Akinlalu *et al.,* 2017; Adiat *et al.,* 2018; Akinlalu *et al.,* 2021). However, some workers are of the opinion that the knowledge–driven models are quite inadequate to assign weights to evidential features (Carranza and Hale, 2002; Porwal *et al.,* 2003; Yousefi and Carranza, 2015). This is because of the inconsistencies associated with the assignment of weights to evidential layers that differ from one expert to another.

In recent years, different studies have been applied using GIS-based data driven models to produce the groundwater potential maps (Madrucci *et al.,* 2008; Prasad *et al*., 2008). In order to prepare the GPM, some studies have applied probabilistic models such as Frequency Ratio (FR) (Oh *et al*., 2011; Razandi *et al*., 2015; Olajide *et al.,* 2022), multi-criteria decision analysis (Chowdhury *et al*., 2009; Rahmati and Melesse, 2016), Weights-of-Evidence (W of E) (Corsini *et al.,* 2009; Lee *et al*., 2012; Ozdemir, 2011; Pourtaghi and Pourghasemi, 2014), Logistic Regression (LR) (Ozdemir, 2011; Pourtaghi and Pourghasemi, 2014), Evidential Belief Function (EBF) (Nampak *et al*., 2014; Pourghasemi and Beheshtirad, 2014; Mogaji *et al*., 2015), Certainty Factor (CF) (Razandi *et al*., 2015), Artificial Neural Network model (ANN) (Lee *et al*., 2012; Adiat *et al.,* 2020). The use of the data–driven method in groundwater potential mapping has been found to be particularly important and has proven to produce excellent results (Nampak *et al*., 2014; Mogaji *et al*., 2015; Adiat *et al.,* 2020) with the entropy method regarded as one of the best models for groundwater potential mapping applicable in different geologic environments in the world especially in a complex environment such as the study area (Jenifer and Jha, 2017).

The data–driven entropy method employs the use of existing data from wells and boreholes to establish a spatial relationship between relevant anomalies which could be obtained from geological, Geographical Information Science (GIS), geophysical and meteorological information (Al–Abadi and Shahid, 2015; Al–Abadi *et al.,* 2016; Jenifer and Jha, 2017). The analysis of the relationship existing between the boreholes or well data and the geospatial anomalies are used in the weight assignment for the generation of groundwater potential map. Though, few study has been aimed at groundwater potential mapping in a complex geological environment using the entropy model, few researchers who have applied this model have found it to be adequate in groundwater potential mapping with good performance index (Al–Abadi and Shahid, 2015; Al–Abadi *et al.,* 2016).

The study area is located in the basement complex, southwestern part of Nigeria where groundwater occurrence is limited

and occurring in pockets of spaces where faults, fractures and joints exist, requiring extensive exploration works. The study area is built up and the lack of space in addition to the complex terrain of the study area makes groundwater exploration especially difficult. In the study area, previous researches using geophysical datasets have been geared towards evaluation of groundwater potential by the analysis and comparison of factors that contribute to groundwater occurrence. However, these factors are arbitrarily analyzed and compared without statistical and mathematical considerations which ensure better output of groundwater potential models. Therefore, there is a need to use conditioning factors related to groundwater occurrence in groundwater potential mapping using a suitable and proven model involving the data–driven entropy method. Hence, this research is aimed at the use of the data–driven entropy model involving conditioning factors such as aquifer resistivity, overburden thickness, coefficient of anisotropy, coefficient of reflection and bedrock topography in the groundwater potential mapping of parts of Ado metropolis.

Location, Geomorphology, Climate and Vegetation of the Study Area

The study area lies at the south western part of Ado Ekiti. It comprises of both state and federal reserved area with inclusion of a new community called Ile-Aanu quarters. Its lies between latitudes 7^0 38' 0''N and 7^0 40' 0''N and longitudes 5^0 10' 0''E and 5^0 12' 0''E in Ado-Ekiti south west, Ado Local Government Area of Ekiti State, Nigeria (Figure 1). The relief of Ado Ekiti is relatively low with isolated hills and inselbergs that are dome-shaped. At the base of these rocks are boulders littering all over the place (Ajayi *et al.*, 2019). The major river draining the area is Ireje River which flows southeast. The river is associated with simple form of minor tributaries.

Geology and Hydrogeology of the Study Area

The geology of Ado-Ekiti belongs to the basement complex rocks of South Western Nigeria. These include coarse grained charnockite, fine grained granite, medium grained-granite and porphyritic biotite-hornblend granite, with superficial deposit of clay and quartzite. Association of the fine-grained charnokite and the porphyritic biotite-hornblende granite suggest a common age (Omotoyinbo, 1994). In the study area, granite and charnockite are the two rocks present (Figure 2). The charnockite ranges in colour from dark-green, to greenish-grey rock with milky quartz and greenish feldspar. The outstanding feature of the coarse grained variety of charnokititic rock in Ado Ekiti is that it is similar to those of Oyawoye (1961, 1965), described as "bauchite" around Bauchi, Nigeria. Other occurrences are in form of small dykes or veins in other granitic rocks. The rock is generally even textured and homogenous with mineral aggregates mainly of biotite and feldspar phenocryst. The superficial deposits are clay, quartzite rubbles and fine sand (SiO_2). The clay is believed to have be formed from the weathering of feldspar mineral present in charnockitic rocks due to alteration of igneous rocks by hydrothermal process and the quartzite rumbles due to high degree of cyclic weathering.

Hydrogeologically, the groundwater potential is quite low owing to the absence of fractures, faults, joints to permit groundwater storage in the study area. Generally, the overburden is relatively shallow within the study area with average of 11m. The groundwater is found within

the overburden and fractured basement while the area is drained by the river Ogbese which flow in the SW–NE direction (Ogundana and Talabi, 2014). Olayinka and Olorunfemi (1992); Ojo *et al.* (2011); Ademilua and Eluwole (2013); Akinlalu *et al.* (2017); Adiat *et al.* (2018); Adiat *et al.* (2020); Akinlalu *et al.* (2021) in different researches in the study area and in similar geologic environment showed that the low groundwater potential in the study area is majorly because of the complex geology in the study area. Furthermore, the basement complex rocks are poor aquifers as they are characterized by low porosity and negligible permeability, resulting from their crystalline nature, thus availability of groundwater resource in such areas can only be attributed to the development of secondary porosity and permeability resulting from weathering and fracturing (Ogundana and Talabi, 2014). Ademilua *et al.* (2017) in a study in the Ado metropolis revealed that five lithologic layers exist in the study area comprising top soil, weathered layer, partly weathered/fractured basement, fractured basement and fresh bedrock. The lithologic units favorable for groundwater storage were observed to be the partly weathered/fractured basement and fractured basement.

Materials and method

Groundwater potential of a particular area is governed by different factors depending on the available datasets and the objective of the study. For this study, conditioning factors involving aquifer resistivity, overburden thickness, overburden resistivity, coefficient of anisotropy, and coefficient of reflection were all obtained from geophysical parameters involving the electrical resistivity method.

The geoelectric data involved the vertical electrical sounding (VES) using the Schlumberger array. A total of twenty eight (28) VES points were occupied in the study area (figure 1). The survey was carried out by gradually expanding the electrode spacing about a fixed center of the array utilizing electrode spread, AB/2 reaching a maximum to 100 m. The field data was subjected to processing involving plotting on a bi–log paper to obtain field curves which are subsequently compared with model curves by running iterations on the WinResist software until a perfect fit is gotten.

The geoelectric parameters obtained from this processing were then used in the calculation and derivation of the first and second order geoelectric parameters that form the conditioning factors for groundwater potential mapping.

Groundwater Potential Conditioning Factors

The groundwater potential conditioning factors used in this study were derived from geophysical parameters by taking into account the first order geoelectric parameters and second order geoelectric parameters (Dar–zarrouk parameter). The groundwater potential conditioning factors used are aquifer resistivity, overburden thickness, coefficient of anisotropy, coefficient of reflection and bedrock topography.

Aquifer Resistivity (AQR)

The aquifer resistivity deals with a parameter that measures the degree of rock resistance (resistivity) to the flow of electric current within a geological formation. The aquifer is any lithologic unit porous and permeable enough to store and transmit water in sufficient quantity. Hence, the response of resistivity measurement over an aquifer unit must be such that the resistivity values must be

relatively low, indicative of the saturation of the lithologic unit delineated as the aquifer. Therefore, resistivity values are used as indirect indices in the determination of aquifer water saturation and thus useful for providing relevant information about groundwater potential of a geological terrain. Low aquifer resistivity inversely correlates with relatively high groundwater occurrence, with the exception of some low permeability rocks, such as clay, which may present low resistivity but poor groundwater quality (Abiola *et al.,* 2009; Akinlalu *et al.,* 2017; Adesola *et al.,* 2021). In the study area, the weathered bedrock and fractured bedrock are delineated as the aquifer units. It is however important to note that not all VES points have aquifer units basically hinged on the relatively high and very low resistivity values of the lithologic units in the subsurface.

Overburden Thickness (OT)

Overburden thickness is estimated as the sum of the thicknesses of the topsoil and the lateritic layer in the respective VES stations. The thicker the unsaturated zone, the higher its capability to retain water from runoff during rainfall and transmit water to the aquifer zone. The unsaturated zone is moderately porous as it contains loose sand particle derived from weathered rocks and other material deposited by wind and runoff water. Areas of thick overburden are often region of comparative groundwater potential than region of less overburden cover, especially where the terrain is less fractured and the overburden material is less clayey (Olorunfemi, 1990; Olorunfemi et al., 1991; Omosuyi et al., 2003; Abdullahi et al., 2016).

Coefficient of Reflection (R_c)

This is an indication of the degree of bedrock fracture of an area. It can also be defined as the ratio of the difference of bedrock resistivity and overlying layer and the sum of both. The reflection coefficient (Rc), of the fresh basement rock of the study area was calculated using the method of Bhattacharya and Patra (1968); Olayinka (1996) and Loke (1999).

The coefficient of reflection is obtained using eq. 1.

$$R_c = \frac{\rho_n - \rho_{n-1}}{\rho_n + \rho_{n-1}} \qquad 1$$

Where ρ_n is the layer resistivity of the nth layer and ρ_{n-1} is the layer resistivity overlying the nth layer. The coefficient of reflection reflects the fracture/resistivity contrast at the fresh basement rock interface, thus providing good insight into the nature of the aquifer in terms of water bearing potential. Often, it is observed that an area of lower reflection coefficient value is indicative of fractured or highly weathered basement, hence translating to high potential of groundwater occurrence (Olayinka, 1996; Oladunjoye *et al.,* 2018). Coefficient of reflection values less than 0.38 are classified as highly fractured basement.

Coefficient of Anisotropy (λ)

The coefficient of anisotropy refers to the degree of inhomegeneity of the subsurface lithology (Adiat *et al.,* 2018), and hence an indirect measure of the degree of fracturing. This implies that the degree of fracturing is an important hydrological index favorable for groundwater storage (Knochenmus and Robinson, 1996). The coefficient of anisotropy is a second order geoelectric parameter calculated from two geoelectric fundamental parameters (layer resistivity, ρ and thickness, h). Other second order geoelectric parameters involving total unit longitudinal conductance, S; total traverse unit resistance, T; average longitudinal resistivity, ρ_l; and average transverse resistivity, ρ_t were used in the computation

of the coefficient of anisotropy as shown in eq. 2–6.

For n layers, the total unit longitudinal conductance is given as

$$S = \sum \frac{h_1}{\rho_1} + \frac{h_2}{\rho_2} + \cdots + \frac{h_n}{\rho_n} \quad 2$$

While the total transverse unit resistance is defined as

$$T = \sum h_1\rho_1 + h_2\rho_2 + \cdots + h_n\rho_n \quad 3$$

The average longitudinal resistivity is calculated from eq. 2 and is given by

$$\rho_l = \frac{H}{S} = \frac{\sum_{i=1}^{n} h_i}{\sum_{i=1}^{n} \frac{hi}{pi}} \quad 4$$

And the average transverse resistivity using eq, 3 is given as

$$\rho_T = \frac{T}{H} = \frac{\sum_{i=1}^{n} h_i\rho_i}{\sum_{i=1}^{n} h_i} \quad 5$$

The coefficient of anisotropy, λ is calculated using eq. 4 & 5 and is given as

$$\lambda = \sqrt{\frac{\rho_l}{\rho_T}} \quad 6$$

Where n is the number of geoelectric layers, ρ is the resistivity of each geoelectric layer and h is the thickness of each geoelectric layer.

The coefficient of anisotropy is a veritable factor for the assessment of groundwater potential of a certain area. Low coefficient of anisotropy value implies low degree of fracturing and thus suggests low groundwater storage potential (Ritzi and Andolsek, 1992; Forson and Whiteman, 2014). Zones of relatively high coefficient of anisotropy implies high degree of fracturing and thus, groundwater potential is high (regions of high lineament/fracture density).

Bedrock Topography (BT)

Bedrock topography is defined as the elevations above mean sea level of the bedrock surface. Bedrock topography is known to affect subsurface water flow and storage. Bedrock topography affects the redistribution of infiltrated water through rivers and lateral subsurface inflow through fractures, among others. This inflow in the subsurface is largely controlled by topography of the bedrock as groundwater flows from high basement elevation to lower basement elevation (Srivastava, 2007). Based on this, bedrock topography was considered as one of the subsurface conditioning factors for groundwater vulnerability in this study. The Bedrock topography, eq. 7, was derived by subtracting the overburden thickness at each VES point from the elevation.

Bedrock topography (BT) = Elevation (m) – Depth to bedrock (m) 7

Groundwater Potential Index

The groundwater potential index of the study area was produced by considering the groundwater conditioning factors involving aquifer resistivity, overburden thickness, coefficient of reflection, coefficient of anisotropy and bedrock topography. These conditioning factors were generated into thematic maps using the inverse distance weighted (IDW) interpolation available on the ArcMap™ software. The IDW was used because it determines cell values using a linearly weighted combination of a set of sample points with the weight being a function of inverse distance. It also controls the significance of known points on the interpolated values based on their distance from the output point (Watson and Philip, 1985; ESRI, 2016). The thematic maps were classified in the GIS environment using natural break to obtain the score in ascending order of each class.

The weight for each thematic map obtained from the data–driven entropy method was multiplied with the scores of each thematic map to obtain the average weight of each thematic layer. The groundwater potential index (GWPI) was produced using the weighted linear combination technique,

based on the concept of a weighted average in which continuous criteria are standardized to a common numeric range, and then combined by means of a weighted average. In simple terms, the GWPI was obtained as a sum of the product of each criterion and its weight as shown in eq. 8. (Drobne and Lisec, 2009).

$$GWPI = \sum_{i=1}^{n} w_i x_i \quad (8)$$

Where w_i is the weight of factor i and x_i is the criterion score or rating of factor i.

The resulting GWPI map produced was subjected to concentration area (C – A) fractal modeling to ensure that classification of groundwater potential index was not done arbitrarily, but in a data–driven way.

Entropy Method

The entropy method is a data – driven approach proposed by Shannon (1948) and modified in recent times by Xu *et al.* (2014); Shevyrev and Carranza (2022). The method determines the weights of thematic layers by assuming that there is set of *m* feasible alternatives, A_i (i = 1,2,…,m) and *n* evaluation criteria C_j (j = 1,2,…,n) in the problem (Aysegul and Esra, 2017). The first step involves forming the decision matrix (eq. 9). The essence is that it shows the performance of different alternatives with respect to various criteria.

$$X = \left(X_{ij}\right)_{m\times n} = \begin{pmatrix} X_{11} & X_{12} & \cdots & X_{1n} \\ X_{21} & X_{22} & \cdots & X_{2n} \\ & \vdots & & \vdots \\ X_{m1} & X_{m2} & \cdots & X_{mn} \end{pmatrix} \quad (9)$$

for i = 1,2…,m; j = 1,2,…,n

Where X_{im} = feasible alternatives

X_{jn} = evaluation criteria

m = number of alternatives

n = number of criteria

The next step involves the evaluation of the normalization of the decision matrix as shown in eq. 10

$$r_{ij} = \frac{x_{ij}}{\sum_{i=1}^{m} x_{ij}} \quad (10)$$

The entropy values are then calculated using eq. 11

$$e_j = -h \sum_{i=1}^{m} r_{ij}\ In\, r_{ij} \qquad i = 1, 2,\ldots\ldots\ldots m;\ j = 1, 2, \ldots\ldots..,n \quad (11)$$

Where $h = \frac{1}{ln(m)}$ (12)

The entropy weight, W_i is calculated as shown in eq. 13

$$e_j = -h \sum_{i=1}^{m} r_{ij}\ In\, r_{ij} \quad (13)$$

Where $\sum_{j=1}^{n} w_j = 1$

Concentration Area (C–A) Fractal Model

Cheng *et al.* (1994) introduced the concentration area fractal model for the evaluation of spatial data in separating background anomalies from anomalies of interest including the discretization and reclassification of anomalies. It describes the relationship between anomalies of an element and the area corresponding to the anomalies. According to the C–A fractal model, an inverse relationship exists between pixels (defined by evidential layer of interest) and area occupied. This relationship can be stated statistically using equation 14.

$$\begin{cases} A(\rho \le v) \alpha \rho^{\alpha 1} \\ A(\rho > v) \alpha \rho^{\alpha 2} \end{cases} \quad (14)$$

Here, A represents the area corresponding to less or greater than the concentration

threshold, ρ represents anomaly values, ν represents the anomaly threshold, ∝ represents proportionality, and α1 and α2 represent the feature indices corresponding to the smallest and largest singularities, respectively. According to fractal theory, the area is a decreasing function of the concentration. In the logarithmic graph of concentration–area fitting, the position where the decreasing slope of the line segment changes suddenly is the fractal threshold.

The singularity (threshold) divides the evidential values into different groups representing different geophysical backgrounds or anomalies. It therefore essentially consists of curves involving the plot of Log (Area) against Log (Transformed evidential values).

Validation

In order to test the efficacy of the groundwater potential index model, validation was done on the groundwater potential model of the study area by using the producing water wells in the study area. Comparison between the water wells and the groundwater potential map was achieved by determining the percentage of correlation using eq. 15

$$\text{Success rate} = \frac{\text{total correlation}}{\text{total number of well data}} \text{ X } 100 \quad 15$$

Results and Discussion

Aquifer Resistivity Map

The aquifer resistivity map of the study area (Figure 3) shows the distribution of resistivity values for the aquifers delineated in the study area. Five classes using the natural break available on the ArcMap™ software was done to classify the resistivity values. The blue color band indicated by dots represents areas that do not have aquifer units basically because the resistivity values are too low in the range of 4 and 90 Ωm showing that the lithologic unit is an aquitard. Also, high resistivity values in the range of 800 and 3000 Ωm falls in the category of areas that are delineated as not being suitable for groundwater potential. This signature of very low resistivity and very high resistivity values is seen to dominate majority of the western flank of the study area. Very low and high resistivity values notably clay and fresh bedrock respectively are indicative of lithologic units having low permeability, hence are translated to lithologic units with poor groundwater potential (Akinlalu *et al.,* 2017; Adiat *et al.,* 2018). This imperatively means that areas in the west flank of the study area do not have potential for groundwater occurrence.

Resistivity values in the range of 112 and 270 Ωm represented by light green color band are indicative of lithologic units that are essentially clayey sand (Figure 3). This signature is seen to dominate majority of the central flank extending to the northern and southern flanks of the study area. The presence of clayey sand in the study area around the central, southern and northern flanks of the study area reduces the potential of groundwater occurrence in the study area due to the presence of clay, reducing groundwater transmissivity. This essentially means that areas in the central, northern and southern flanks of the study area have low potential for groundwater occurrence. High groundwater occurrence having resistivity values in the range of 270 and 785 Ωm represented by yellow, amber and red color bands are observed to have sparse occurrences in the study area, notably in the eastern flank of the study area. This signature is seen to be extensive especially around VES7, VES5 and VES4. The moderate resistivity values observed in those areas are indicative of fractured and highly weathered basement rocks,

permitting ground water occurrence in the study area. Majority of the areas delineated as having high groundwater potential based on the resistivity values are seen to coincide with granitic rocks (Figures 2 & 3). This is with the exception of a pocket of moderate resistivity value where VES8 is located, occurring spatially with charnockitic rocks in the study area (Figures 2 & 3) which is generally known to have low groundwater potential owing to the nature and composition of the rock unit essentially made up of clay. This is confirmed as majority of areas having no and low groundwater potential are spatially linked to the occurrence of charnockitic rocks in the study area. This essentially means that charnockite have low groundwater potential and granitic rocks have high groundwater potential especially if they are fractured, faulted and highly weathered. Therefore, areas in the eastern flank of the study area especially in regions around VES7, VES5, VES4 and VES1 in the southern flank of the study area have potential for groundwater occurrence.

Overburden Thickness

The overburden thickness map of the study area (Figure 4) shows the distribution of lithologies involving the top soil and lateritic layer in the study area. The overburden thickness map is divided into five distinct classes based on the thicknesses of the overburden unit in the study area. Very thin overburden thickness (1–2.85 m), thin overburden thickness (2.85–3.96 m); moderately thick overburden (3.96–5.52 m); thick overburden (5.52–8.34 m) and very thick overburden (8.34–13.4 m). The importance of overburden thickness in groundwater occurrence of a region cannot be overestimated as thick overburden ensures increased groundwater storage and subsequent percolation into aquifer units if available (Adiat *et al.,* 2018). Conversely, thin overburden reduces groundwater potential because groundwater storage also reduces, thus, having direct effect on groundwater recharge into aquifer units (Abiola *et al.,* 2009; Akinlalu *et al.,*2017; Adiat *et al.,* 2018).

Based on the classifications on Abiola *et al.* (2009); Adiat *et al.,* (2018); Adesola *et al.* (2021), overburden units having thickness in the range of 0.1 to 4 m are considered to decrease groundwater potential significantly while overburden thickness greater than 10 is considered to significantly enhance groundwater potential of a region. Hence, a close look at the overburden thickness map shows that the study area is almost entirely dominated by thin overburden indicated by green, light green and yellow color bands (1–5.52 m), indicating that the study area has essentially poor groundwater potential. This signature is observed to have major expressions in the northern flank of the study area with an increased extension to the southern flank of the study area. There also concentric like anomalies in the western and eastern flanks of the study area.

This effectively means that there would be very low groundwater storage in the areas with green, light green and yellow color bands basically because groundwater storage would be low and subsequently lead to reduced groundwater recharge of the aquifer units in the area. This explains why majority of the area with thin overburden coincide spatially with areas delineated as not having aquifer units especially in the northern and western flanks of the study area especially around VES9, VES12, VES23, VES27, VES26, VES25, VES24 and VES20 (Figures 3 & 4).

A general look at the overburden thickness map shows that the occurrence of the bedrock is shallow in the study area as the overburden thickness is relatively thin with a thickness range of 1 and 13.4 m. This implies that groundwater storage in the study area will be low as the relatively thin overburden units would not permit groundwater storage. However, relatively thick overburden thickness is observed as concentric anomaly in the western flank and eastern flanks of the study area around VES28 and VES18 with areas of moderate overburden thickness in the northern, western and southern flanks of the study area around VES7, VES21, VES18 and VES2. These areas have high groundwater potential since groundwater storage would increase which would in turn increase groundwater recharge into aquifer units present in those areas (Abiola *et al.,* 2009; Akinlalu *et al.*,2017; Adiat *et al.,* 2018; Adesola *et al.,* 2021). This explains why aquifer units are also delineated in those areas with relatively thick overburden (Figures 3 & 4).

Generally, the overburden in the study area is thin. The implication of this is that groundwater occurrence in the study area will be susceptible to groundwater contamination. This is majorly because the lack of thick overburden units to serve as protective cover and natural filter for groundwater would mean that runoff water from rainfall that are contaminated included contaminant plumes from landfills, dumpsites and industrial wastes would find its way into aquifer units (Abiola *et al.,* 2009).

Coefficient of Reflection

The coefficient of reflection map of the study area (Figure 5) shows coefficient of reflection values range between 0.0187 and 0.9054. The coefficient of reflection values of the study area are divided into five classes depicting the range and variation of anomalies in the study area. The anomalies are divided into very low (0.0187–0.2379); low (0.2379–0.3665); moderate (0.3665–0.4812); high (0.4812–0.6238); very high (0.6238–0.9054). Very low and low coefficient of reflection values represented by green and light green color bands respectively are seen to occupy majority of the northern and central flanks of the study area with patches in the western and southern flanks of the study area. This signature is indicative of high degree of fracturing of the bedrock and is a strong index of high groundwater potential in those areas. This is because fracturing creates pockets of spaces in rocks, allowing groundwater infiltration and storage. Hence, regions in the northern and central flanks of the study area with patches in the western and southern flanks of the study area around VES26, VES8, VES9, VES12, VES11, VES6, VES5, VES20, VES23, VES16 and VES3 have high potential for groundwater occurrence (Figure 5). However, most of the VES points are not located in areas of groundwater potential delineated from the aquifer resistivity with the exception of VES5 and VES8. This shows that groundwater occurrence in the study area are majorly not as a result of fracturing, but from thick overburden as all the aquifer units coincide with areas of relatively thick overburden (Figures 3, 4 & 5).

A general look at the coefficient of reflection map of the study area shows that majority of the study area is not fractured. Coefficient of reflection values in the range of 0.3665 and 0.9054 represented by yellow, amber and red color bands are observed to have strong expression in the western, southern and patches in the northern flanks of the study area. This is

indicative of the low groundwater potential of the study area.

Coefficient of Anisotropy

The coefficient of anisotropy map (Figure 6) shows the anisotropic values ranging from 1.0002 to 2.1295 obtained in the study area. It shows the degree of fracturing of lithologic units in the study area with the classification as regards groundwater potential done based on Adiat *et al.* (2018). Very low groundwater potential represented as green color band (1.0002–1.508); low groundwater potential represented as light green color band (1.508–1.2527); moderate groundwater potential represented as yellow color band (1.2527–1.4077); high groundwater potential represented as amber color band (1.4077–1.6645) and very high groundwater potential represented as red color band (1.6645–2.1295) (Figure 6) were obtained using the natural break classification available on the ArcMap™ software.

Figure 6 shows that the groundwater potential of the study area is generally low as most of the areas have low degree of fracturing. This is indicated by the dominance of very low and low coefficient of anisotropy dominating majority of the study area with major expression in the northern, western and southern flanks of the study area. These areas also spatially coincide with areas with low groundwater potential delineated from the aquifer resistivity and coefficient of reflection maps (Figures 3, 4, 5 & 6). However, areas of low coefficient of anisotropy coincide spatially with areas of relatively thick overburden and aquifer units around VES2, VES7 and VES21, indicating that the groundwater occurrence in those areas are not as a result of fracturing, but majorly because of groundwater storage as a result of the relatively thick overburden in those areas (Figures 3, 4 & 6). This also affirms the observation made from the coefficient of reflection map (Figure 5).

In the same vein, moderate to very high groundwater potential as a result of the high degree of fracturing with coefficient of anisotropy in the range of 1.2527 and 2.1295 are observed to have major occurrences in the central flank of the study area with patches in the northern, western and southern flanks of the study area. These regions are expected to have high groundwater potential since the rock units are highly fractured in the area, permitting groundwater infiltration, migration and storage into aquifer units. This signature is observed to correlate spatially with areas delineated as having high potential of groundwater occurrence especially in the central and southern flanks of the study area around VES5 and VES1 (Figures 3, 5 & 6). Furthermore, the high degree of fracturing especially in the central and southern flanks of the study area coinciding with the occurrence of granitic rocks indicate there is a high degree of tectonism on the granitic rocks relative to charnockitic rocks in the study area. Hence, groundwater potential would be higher in areas with granite occurrence than in areas with charnockite occurrence in the study area.

Bedrock Topography

The bedrock topography map (Figure 7) shows the bedrock relief of the study area with range in the value of 402.4–458.8 m. Water flows from areas of high gradient to areas of low gradient, thus making the bedrock topography a good index in assessing the groundwater potential of an area. Classification done using the natural break available of the ArcMap™ software divided the map into very low relief represented by green color band (402.4–417 m); low relief represented by light

green color band (417–425.2 m); moderate relief represented by yellow color band (425.2–432.5 m); high relief represented by amber color band (432.5–440.9) and very high relief represented by red color band (440.9–458.8 m).

The very low and low relief signature with expression in the northern flank of the study area extending to the central flank of the study area with a circular patch in the southern flank of the study area (figure 7) is indicative of areas of groundwater accumulation, hence high potential of groundwater occurrence. This is because those zones are at a lower altitude relative to other areas, thus permitting the accumulation of water that may eventually find their ways into cracks, crevices, fractures and faults especially if the area is tectonically active. However, comparison of the bedrock topography map with other groundwater conditioning factors show that those areas do not coincide with areas of high groundwater potential delineated from the aquifer resistivity, coefficient of reflection and coefficient of anisotropy maps of the study area (Figures 3, 5 & 6) with the exception of areas around VES21, VES22 & VES28.

This is because the area is not tectonically active to allow seepages of accumulated water into aquifer units to enable storage, thus effectively limiting the groundwater potential of the areas. This means that areas around VES21, VES22 & VES28 have high potential and groundwater potential.

Furthermore, high bedrock relief in the range of 425.2–458.8 m is seen to have a strong expression in the southern flank of the study area with patches of occurrence in the northern and western flanks of the study area (Figure 7). Due to the high gradient in these areas, water would most like flow away from the region to areas of low gradient, translating to low groundwater potential. However, comparison of the bedrock topography map with the coefficient of reflection and coefficient of anisotropy maps indicates that areas with high bedrock topography spatially coincide with areas that are highly fractured especially around VES5, VES4, VES26, VES25, VES23, VES18, VES1, VES2, VES3, VES17, VES8, VES9, VES24 & VES27 (Figures 5, 6 & 7). This is because the presence of fracture allowed the infiltration of water before they are transported to areas of low relief, though the groundwater potential in the area would be low because little water would be available for seepage into fractured basement rocks.

This implies that areas with high fracture density occurring spatially with areas of low bedrock relief increases groundwater potential.

Weight Assignment using the Data–Driven Entropy Method

The objective method of assigning weights to groundwater potential conditioning factors using the entropy method was utilized in this study. Groundwater conditioning factors involving aquifer resistivity, overburden thickness, coefficient of reflection, coefficient of anisotropy and bedrock topography were weighted to assess the contribution of each factor to groundwater potential modeling.

The weighting assignment calculation using the entropy method as shown in Tables 1, 2 & 3 showed that aquifer resistivity has the highest rating with 0.6338. This is closely followed by overburden thickness with weight rating 0.1865; coefficient of reflection with weight rating of 0.1612; coefficient of anisotropy with weight rating of 0.0180; bedrock topography with weight rating of 0.0004 (Tables 3 & 4).

The aquifer resistivity with a weight of 0.6338 has the highest contribution to groundwater potential modeling. This is because the resistivity values indicate the suitability of the lithologic units to groundwater accumulation in terms of fracturing and lithology type, making aquifer resistivity to be the most important groundwater conditioning factor.

The overburden thickness has the next importance and contribution to groundwater potential modeling in this study, majorly because of its direct contribution to groundwater recharge. Furthermore, the weight assignment of coefficient of reflection and coefficient of anisotropy as indices of heterogeneity and fracturing of the basement rocks indicate that they are respectively the third and fourth most important criteria in groundwater potential modeling in the study area. This is because it is possible for fracturing to occur in basement rocks without having high groundwater potential. This is because the groundwater potential of a fractured basement is hinged on rechargeability, density of fractures and lithology. Therefore, if an area is highly fractured from the analysis of the coefficient of anisotropy and coefficient of reflection, but has low recharge rate, poor fracture density to enhance migration of fluids and lithology to permit groundwater storage and transmissivity, the groundwater potential of such as area would be low. The bedrock topography has the least contribution to groundwater potential in the study area with a weight assignment of 0.0004. This shows that it is possible for the bedrock relief of a certain area to be low such that groundwater is accumulated there, but having low groundwater potential. This is because lack of fracturing and permissible lithology would not permit the infiltration of water for storage leading to poor groundwater potential.

Groundwater Potential Map of the Study Area

The groundwater potential map of the study area produced from the integration of the weights of groundwater conditioning factors has fuzzy scores range from 0.0041 to 0.970 reflecting the groundwater potential index of the study area (Figure 8a). The map shows that the western flank of the study area has low ground potential while the eastern flank of the study area has relatively high potential of groundwater potential with an isolated anomaly in the northern flank of the study area.

The classification of the groundwater potential map using the concentration area (C–A) fractal model divided the map into five anomalies based on the importance to groundwater potential. The classifications are background (green color band); low (tourmaline green color band); moderate (yellow color band); high (amber color band) and very high (red color band). The background anomaly basically reflect areas with no groundwater potential indicating that the groundwater conditioning factors have scores of 1 (Table 4), hence, no significance to groundwater potential. This anomaly is observed in the northern flank of the study area around VES9, VES12, VES14 and VES13; western flank of the study area around VES15, VES23, VES27, VES 25, VES26 and VES24 with patches in the southern flank of the study area around VES20 and VES17. This shows that those areas are not suitable for groundwater extraction and development. That explains the limited number of wells located in those regions (Figure 8c).

Low groundwater potential is seen to dominate majority of the western flank of

the study area, bearing spatial correlation with the occurrence of mostly charnockite. The occurrence of charnockite could have been responsible for the low groundwater potential in the area, majorly because charnockite weathers to form clay which is a poor lithologic unit for groundwater potential. The spatial correlation with areas having granite occurrence around VES19, VES16, VES1, VES2 and VES3 could be as a result of the low tectonic activity that would have caused fracturing of rocks in those areas (Figures 2, 6 & 8c). The occurrence of moderate groundwater potential especially in the northern flank of the study area branching to the southern flank of the study area shows that the groundwater conditioning factors in those regions have moderate contribution to groundwater potential (Figure 8c). This anomaly is a strong reflection of the varying degrees of contribution of the groundwater conditioning factors employed in this study to groundwater potential in the regions. It is seen that this anomaly corresponds majorly with the occurrence of granite in the western flank of the study area.

High and very high groundwater potential is observed majorly in the northern and central flanks of the study area with patches in the southern flank of the study area. This anomaly shows that all the groundwater conditioning factors used in this study have at least high score of groundwater potential index in the region mapped.

The occurrence of very high groundwater potential with areas of granite occurrence shows that granite in the area is the lithologic unit that permits groundwater accumulation and storage (Figure 9). The occurrence of high groundwater potential in areas of charnockite occurrence could be as a result of the intense fracturing that has occurred in the area especially around VES11and VES28 (Figures 5 & 8c). Also, the low bedrock relief around VES11 coupled with the high fracture density delineated from the coefficient of reflection map (Figures 5, 7 & 8c) could be responsible for the high groundwater potential anomaly observed over the charnockite in the study area.

Generally, overlay of the classified groundwater potential map with the geological fabrics of the study area shows that areas of moderate and very high groundwater potential have spatial correlation with the occurrence of granite with very few correlations in areas of charnockite occurrence in the northern and central flanks of the study area around VES8, VES11, VES6, VES5 and VES28. This is a strong indication that granite in the study area supports the groundwater potential conditioning factors used for this study, and therefore has relatively good potential for groundwater occurrence.

Validation

The locations of twelve (12) wells were matched with the classified groundwater potential map of the study area. The location of water wells in the study area correlates well with areas of moderate to very high groundwater potential of the study area with 75% accuracy (Table 5). This shows that the groundwater potential model generated for the study area is suitable for evaluating the groundwater potential of the study area. It can also serve as guide for groundwater developers on groundwater development in the study area. Since nine of the twelve water wells fall in areas of high and very high groundwater potential area, therefore, this model can be employed as a guide for water developers in groundwater potential mapping and development in similar geologic environments of the world.

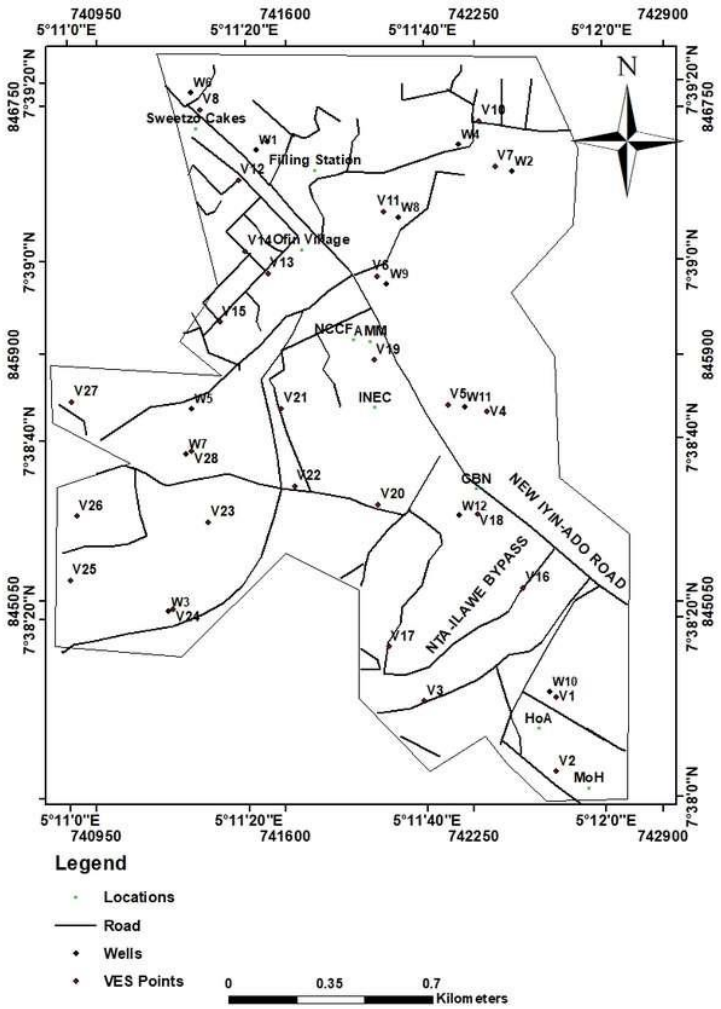

Figure 1: Location Map of the Study Area.

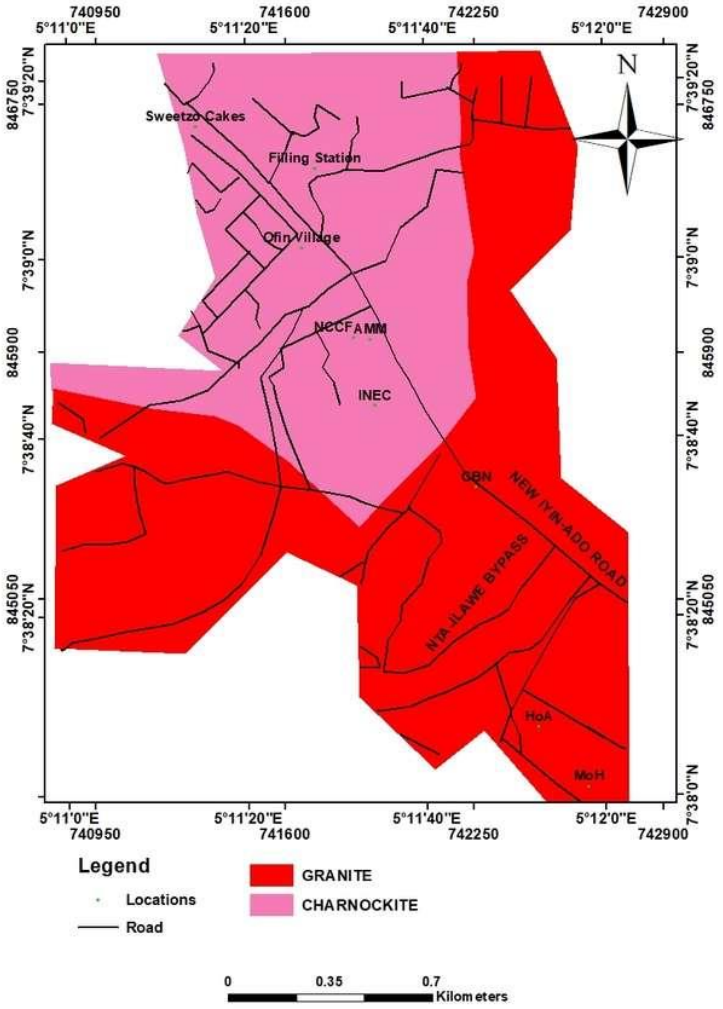

Figure 2: Geological Map of the Study Area (Modified after Ajayi *et al.*, 2019).

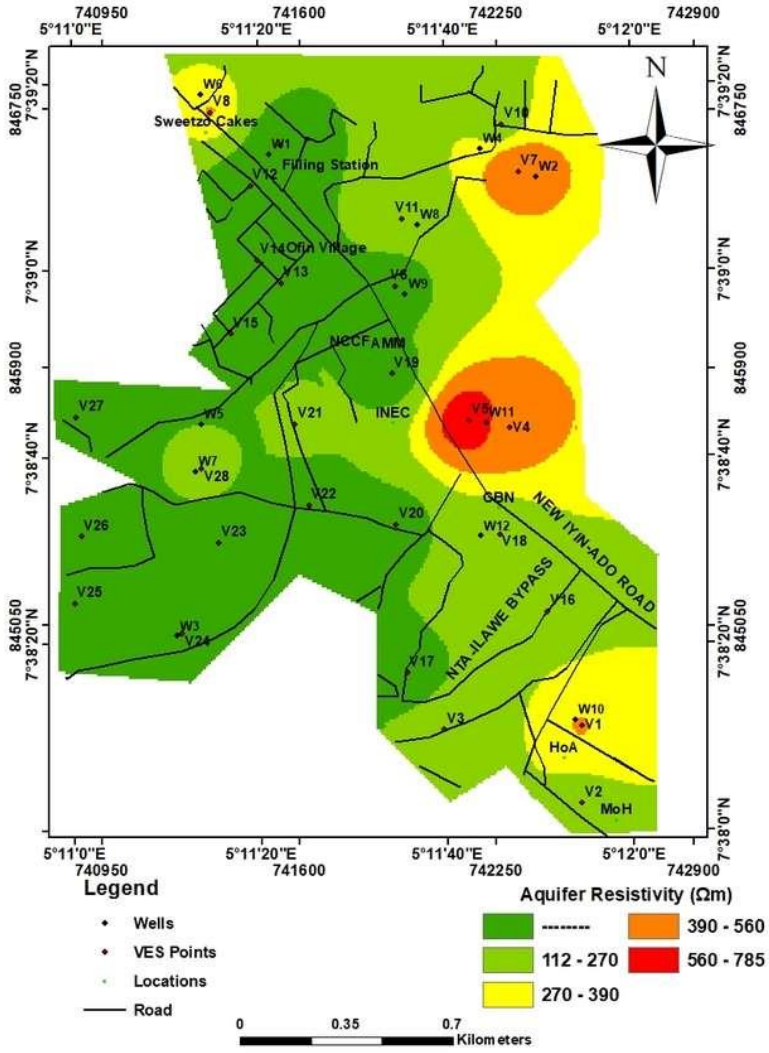

Figure 3: Aquifer Resistivity Map of the Study Area.

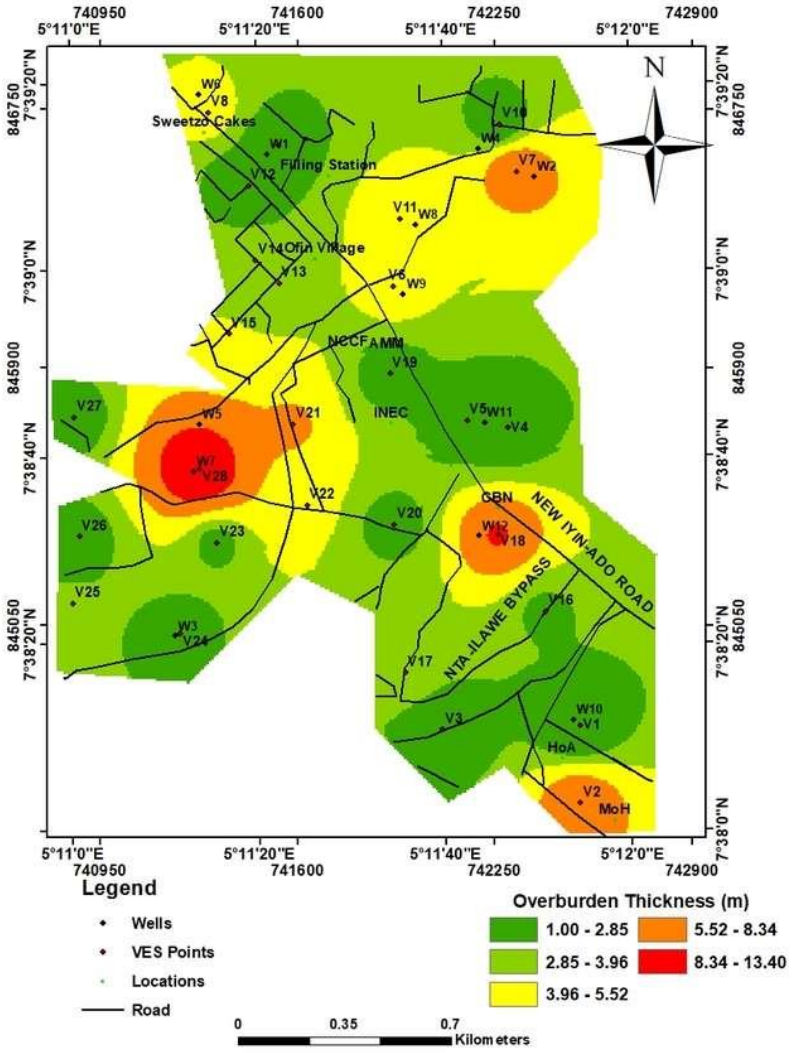

Figure 4: Overburden Thickness Map of the Study Area.

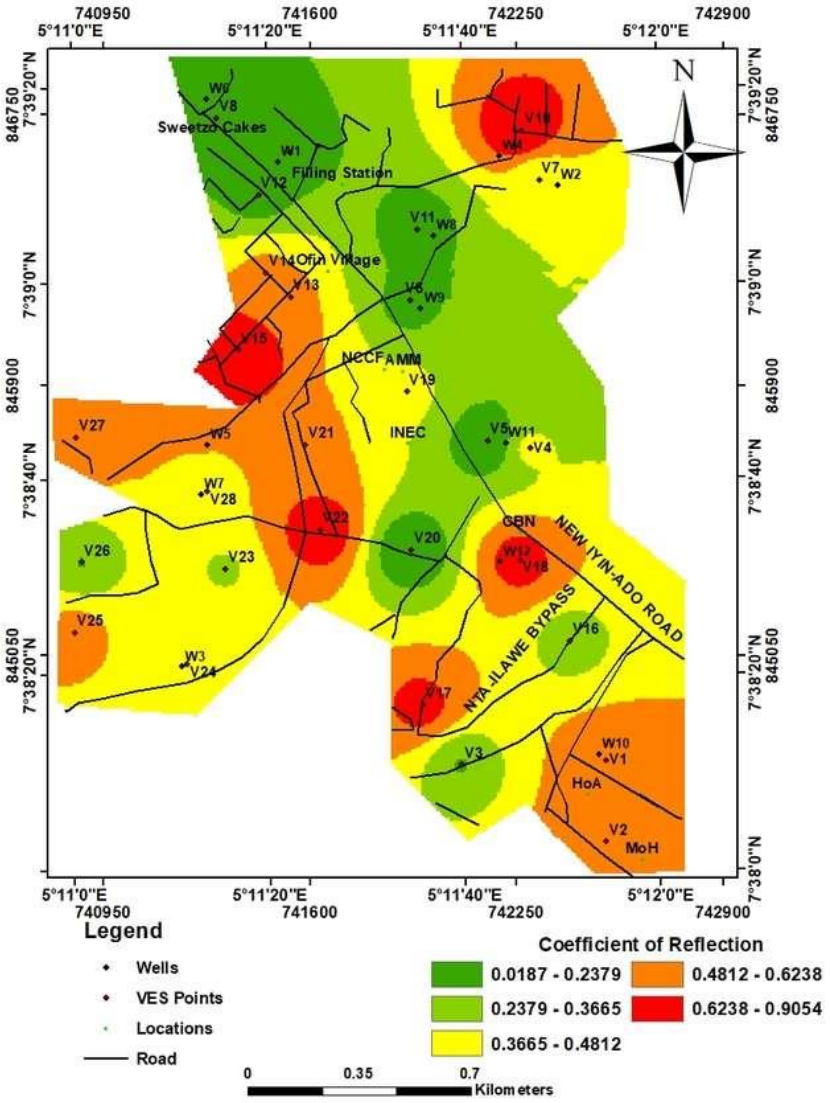

Figure 5: Coefficient of Reflection Map of the Study Area.

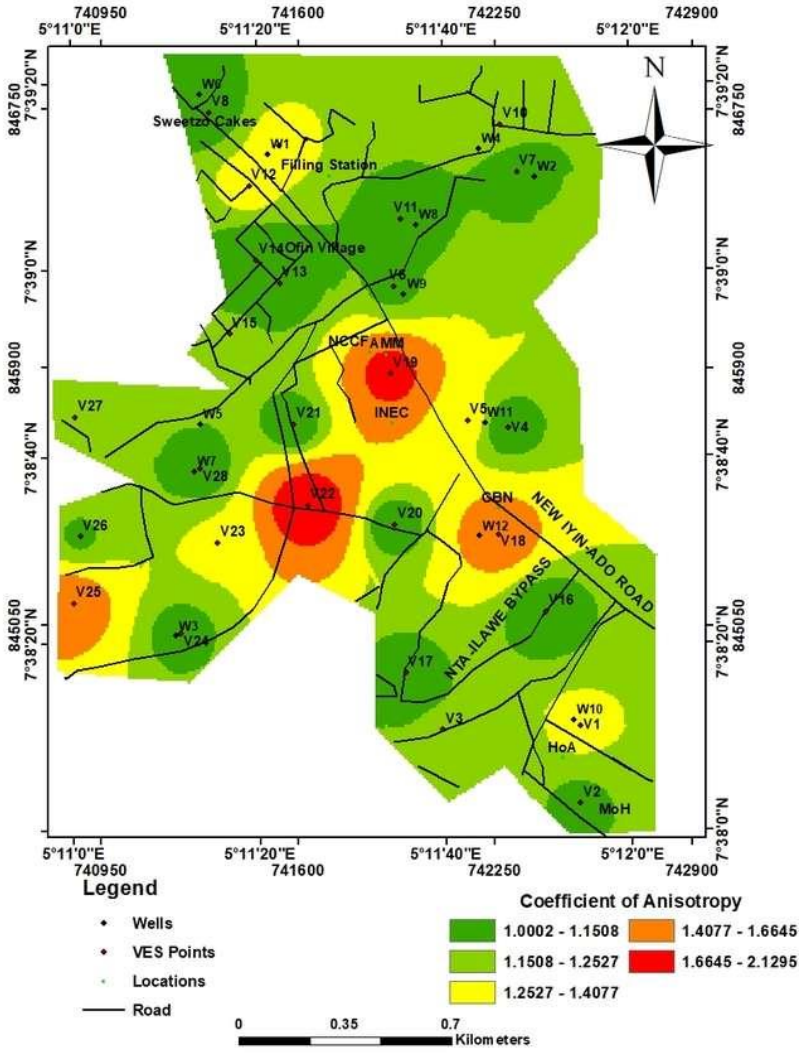

Figure 6: Coefficient of Anisotropy Map of the Study Area.

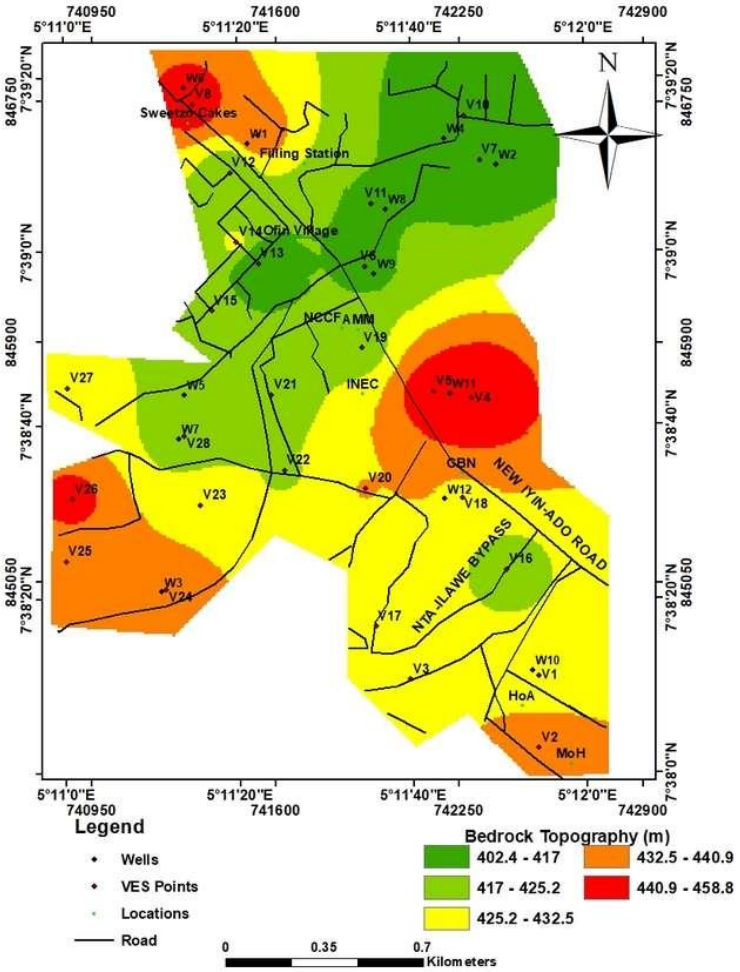

Figure 7: Bedrock Topography Map of the Study Area.

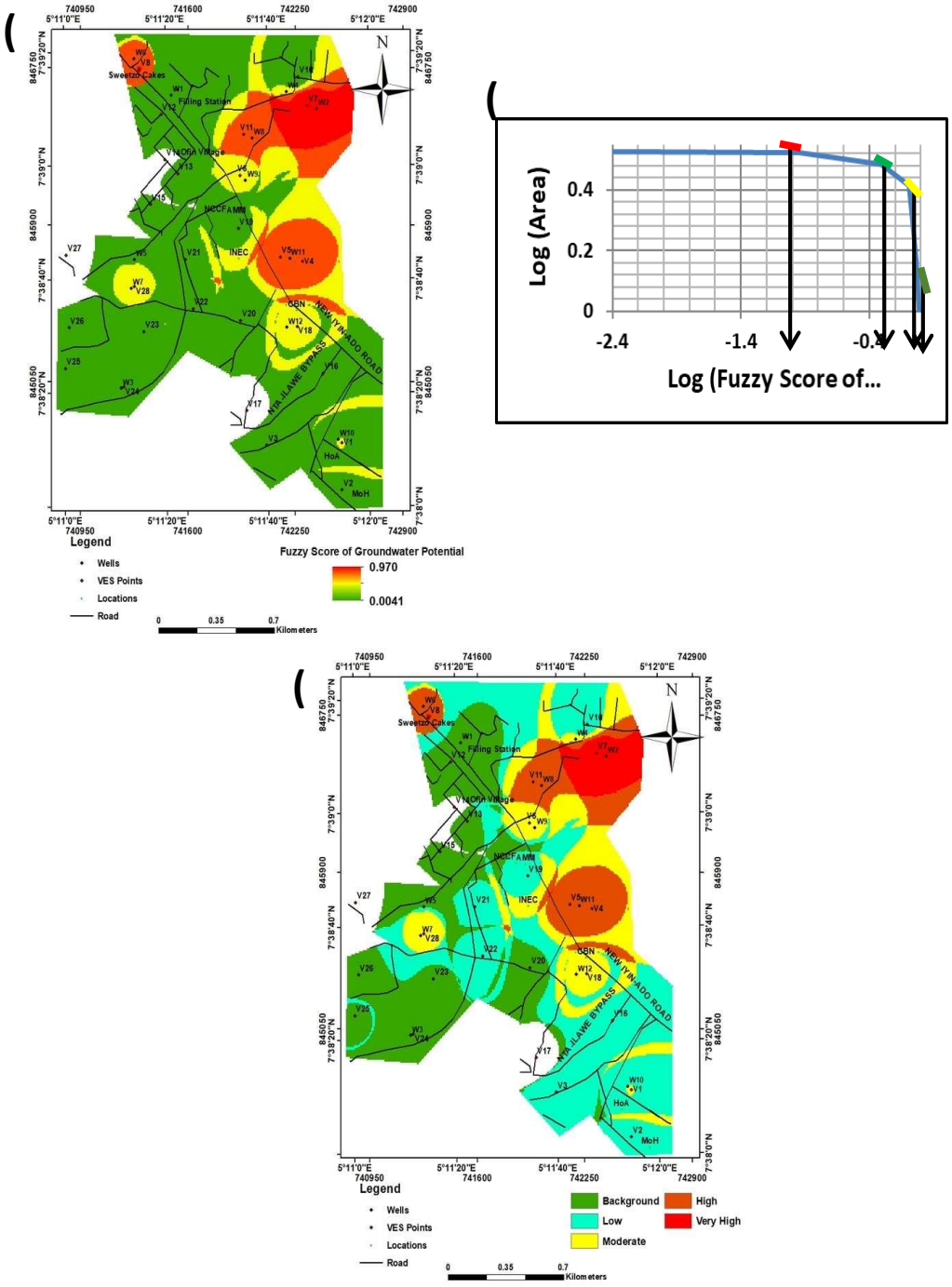

Figure 8: (a) Fuzzified Groundwater Potential Map of the Study Area (b) Concentration Area (C–A) Fractal Model of the Groundwater Potential Fuzzy Scores (C) Classified Groundwater Potential Map of the Study Area.

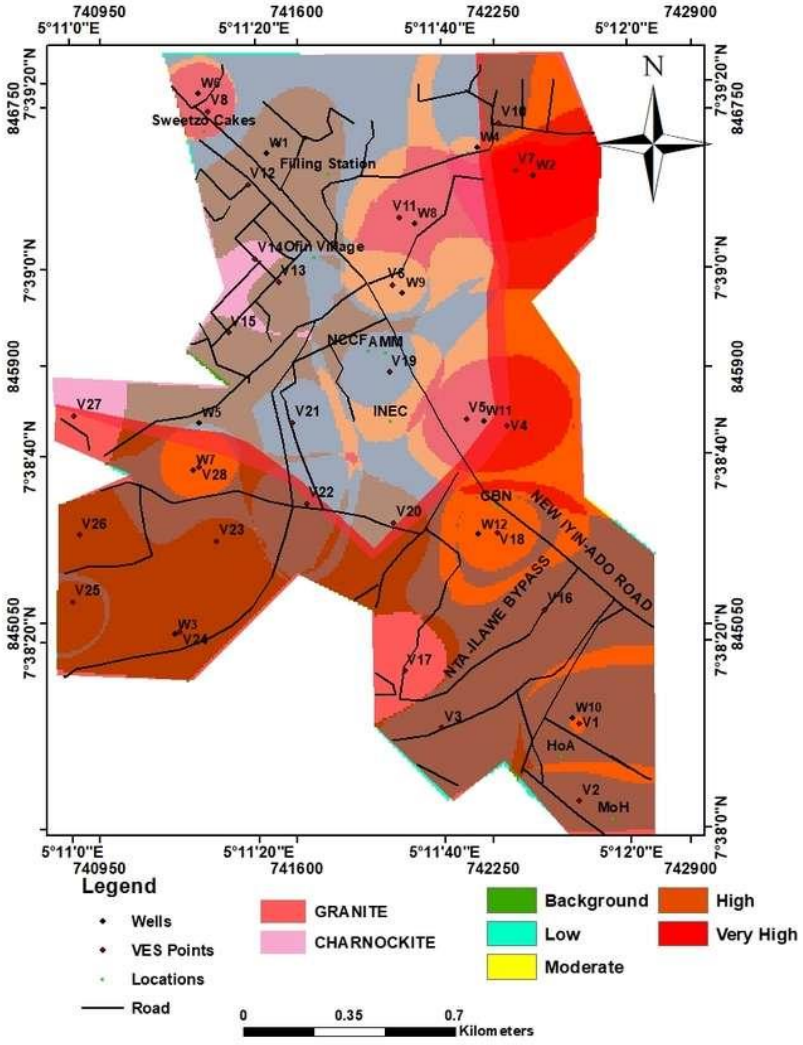

Figure 9: Overlay of the Classified Groundwater Potential Map and Geological Map of the Study Area.

Table 1: Decision Matrix for Groundwater Potential Conditioning Factors

VES NO	Aquifer Resistivity	Overburden Thickness	Coefficient of Reflection	Coefficient of Anisotropy	Bedrock Topography
1	395	1	0.5825	1.3029	427.2
2	236	7.3	0.6181	1.1204	438.1
3	199	1.3	0.2317	1.1586	431
4	475	1.4	0.3961	1.0144	458.8
5	785	1.7	0.0663	1.3282	448.3
6	–	5	0.1685	1.1045	413.5
7	542	7.3	0.3661	1.1034	410.7
8	394	4.9	0.0187	1.0163	449.6
9	–	1.6	0.1492	1.3499	439.6
10	207	1.6	0.8431	1.2069	402.4
11	200	5.3	0.1204	1.0654	415.7
12	–	1.5	0.1308	1.3531	417.7
13	112	3.4	0.5372	1.0115	403.9
14	112	3	0.5274	1.0099	427.3
15	–	4	0.9054	1.1838	420.5
16	238	2.5	0.2938	1.0002	419.1
17	–	3.9	0.6985	1.0661	427.6
18	172	8.7	0.7286	1.6403	431.3
19	–	1.7	0.4021	1.8818	421.1
20	–	1.8	0.0309	1.0122	432.6
21	155	5.9	0.5394	1.0114	421.1
22	–	4.3	0.8017	2.1297	424.1
23	–	2.2	0.3463	1.2170	430.7
24	–	2	0.4171	1.0721	438.5
25	–	2.9	0.5357	1.6028	436.3
26	–	1.9	0.2353	1.1239	444.9
27	–	1.8	0.5924	1.2095	429.4
28	193	13.4	0.4062	1.0242	417.6
$\sum_{j=1}^{m} X_{IJ}$	4415	103.3	11.6895	34.3745	11978.6

Table 2: Normalized Decision Matrix for Groundwater Conditioning Factors

VES NO	Aquifer Resistivity	Overburden Thickness	Coefficient of Reflection	Coefficient of Anisotropy	Bedrock Topography
1	0.089468	0.009681	0.049831	0.037902	0.035664
2	0.053454	0.070668	0.052877	0.032594	0.036574
3	0.045074	0.012585	0.019821	0.033704	0.035981
4	0.107588	0.013553	0.033885	0.029511	0.038302
5	0.177803	0.016457	0.005672	0.038639	0.037425
6	–	0.048403	0.014415	0.032131	0.03452
7	0.122763	0.070668	0.031319	0.032098	0.034286
8	0.089241	0.047435	0.0016	0.029566	0.037534
9	–	0.015489	0.012764	0.039271	0.036699
10	0.046886	0.015489	0.072125	0.035109	0.033593
11	0.0453	0.051307	0.0103	0.030994	0.034704
12	–	0.014521	0.01119	0.039364	0.034871
13	0.025368	0.032914	0.045956	0.029426	0.033718
14	0.025368	0.029042	0.045117	0.02938	0.035672
15	–	0.038722	0.077454	0.03444	0.035104
16	0.053907	0.024201	0.025134	0.029096	0.034987
17	–	0.037754	0.059754	0.031014	0.035697
18	0.038958	0.084221	0.062329	0.04772	0.036006
19	–	0.016457	0.034398	0.054743	0.035154
20	–	0.017425	0.002643	0.029447	0.036114
21	0.035108	0.057115	0.046144	0.029423	0.035154
22	–	0.041626	0.068583	0.061957	0.035405
23	–	0.021297	0.029625	0.036976	0.035956
24	–	0.019361	0.035682	0.03119	0.036607
25	–	0.028074	0.045827	0.046629	0.036423
26	–	0.018393	0.020129	0.032697	0.037141
27	–	0.017425	0.050678	0.035185	0.035847
28	0.043715	0.129719	0.034749	0.029796	0.034862

Table 3: Entropy Values, Degree of Divergence and Entropy Weights for Groundwater Conditioning Factors

	Aquifer Resistivity	Overburden Thickness	Coefficient of Reflection	Coefficient of Anisotropy	Bedrock Topography
Entropy Values, e_{ij}	0.762457	0.930103	0.939594	0.993248	0.999856
$d_{ij} = (1 - e_{ij})$	0.237543	0.069897	0.060406	0.006752	0.000144
Entropy Weights, W_{ij}	0.6338	0.1865	0.1612	0.0180	0.0004

Table 4: Rating and Weighting for Groundwater Conditioning Factors

Conditioning Factors	Category (Classes)	Groundwater Potential	Rating	Weight
Aquifer Resistivity	<112 & >785 Ωm	No	0	0.6338
		Low	2	
	112–270 Ωm	Moderate	3	
	270–390 Ωm	High	4	
	390–560 Ωm	Very High	5	
	560–785 Ωm			
Overburden Thickness	1.00–2.85 m	Very Low	1	0.1865
	2.85–3.96 m	Low	2	
	3.96–5.52 m	Moderate	3	
	5.52–8.34 m	High	4	
	8.34–13.40 m	Very High	5	
Coefficient of Reflection	0.0187–0.2379	Very High	5	0.1612
	0.2379–0.3665	High	4	
	0.3665–0.4812	Moderate	3	
	0.4812–0.6238	Low	2	
	0.6238–0.9054	Very Low	1	
Coefficient of Anisotropy	1.0002–1.1508	Very Low	1	0.0180
	1.1508–1.2527	Low	2	
	1.2527–1.4077	Moderate	3	
	1.4077–1.6645	High	4	
	1.6645–2.1295	Very High	5	
Bedrock Topography	402.4–417.0 m	Very High	5	0.0004
	417.0–425.2 m	High	4	
	425.2–432.5 m	Moderate	3	
	432.5–440.9 m	Low	2	
	440.9–458.8 m	Very Low	1	

Table 5: Correlation of Water Wells with Groundwater Potential Anomalies

Pits	Easting	Northing	Background	Low	Moderate	High	Very High
Well 1	741498	846600	✔			✔	Failed
Well 2	742378	846527				✔	Passed
Well 3	741196	845015	✔				Failed
Well 4	742193	846619				✔	Passed
Well 5	741276	845711	✔				Failed
Well 6	741272	846799			✔		Passed
Well 7	741258	845557				✔	Passed
Well 8	741988	846369			✔		Passed
Well 9	741948	846141			✔		Passed
Well 10	742510	844741				✔	Passed
Well 11	742216	845718			✔		Passed
Well 12	742199	845345					Passed

% of Agreement = 9/12 * (100) = 75%

Conclusion

In this study, the groundwater potential map of a typical basement complex environment, southwestern Nigeria was done. This was achieved by combining groundwater conditioning factors involving aquifer resistivity, overburden thickness, coefficient of reflection, coefficient of anisotropy and bedrock topography obtained from electrical resistivity data. These groundwater conditioning factors were assigned weights using the entropy method which is an objective way of assigning weights to evidential layers. The weight assignment shows that aquifer resistivity has the highest contribution to groundwater potential in the study area. This is followed by overburden thickness, coefficient of reflection, coefficient of anisotropy and bedrock topography respectively. The integration of these groundwater conditioning factors using their respective weight was used in generating the groundwater potential map of the study area.

The groundwater potential map was classified into five classes using the

concentration area (C–A) fractal model consisting of background, low, moderate, high and very high potential. The study showed that majority of the western flank of the study area have background and low potential of groundwater occurrence. Furthermore, these areas coincide majorly with the occurrence of charnockite in the study area. Whereas, areas in the northern, central and eastern flank in the study area have moderate to very high potential of groundwater occurrence, also coinciding with the occurrence of granite in the study area.

The study validated the groundwater potential model with water wells indicating a 75% agreement which is quite a strong expression of the success of the produced model. The groundwater potential map shows that granite in the study area has experienced intense tectonic activity than the charnockite in the study area. This explains why majority of the water wells coincide with areas of high and very high groundwater potential in areas of granite occurrence. Therefore, groundwater exploration is advised to be concentrated majorly in the eastern flank of the study area where there are granite occurrences.

Conflict of Interest

The corresponding author on behalf of the authors declares no conflict of interest.

References

Abdullahi, M., Yelwa, N., Abdulmumin, A.and Nabage, N.A. (2016). Groundwater exploration in the Basement Complex around Chibok area in Northeastern Nigeria using vertical electrical sounding method. *Nigerian Journal of Basic and Applied Sci*ence 24(2):37–44.

Abiola, O., Enikanselu, P. A. and Oladapo, M. I. (2009). Groundwater potential and aquifer protective capacity of overburden units in Ado-Ekiti, southwestern Nigeria. *International Journal of Physical Sciences*, *4*(3), 120–132.

Ademilua, O.L. and Eluwole, A.B. (2013). Hydrogeophysical evaluation of the groundwater potential of Afe Babalola University, Ado Ekiti, Southwestern Nigeria, *Journal of Emerging Trends in Engineering and Applied Sciences* 4(1): 77–83.

Ademilua, O.L., Ojo, O.F., Eluwole, A.B. and Ajayi, C.A. (2017). Geophysical investigation for aquifer potential assessment and groundwater development at EKSU staff quarters GRA Ado Ekiti, Southwest Nigeria. *Journal of Environment and Earth Science* 7(2): 1–15.

Adepelumi, A.A., Yi, M.J., Kim. J.H. and Ako, B.D. (2006). Integration of surface geophysical methods for fracture detection in crystalline bedrocks of southewestern Nigeria. *Journal of Hydrology* 14:1284–1306.

Adesola, B.M., Abdul–Nafiu, A.K., Adewale, A.A., Olubusola, I.S., Omowonuola, A.K., Omang, B.O., Akinola, O.A., Gregory, O.O. and Issac, A. (2021). Groundwater sustainability and the divergence of rock types in a typical crystalline basement complex region, southwestern Nigeria. *Turkish Journal of Geosciences* 2(1), 1–11. https://doi.org/10.48053/turkgeo.777217.

Adiat, K.A.N., Nawawi, M.N.M. and Abdullah, K. (2012). Assessing

the accuracy of GIS-based elementary multi criteria decision analysis as a spatial prediction tool—a case of predicting potential zones of sustainable groundwater resources. *Journal of Hydrology* 440–441:75–89. https://doi.org/10.1016/j.jhydrol.2012.03.028.

Adiat, K.A.N., Nawawi, M.N.M. and Abdullah, K. (2013). Application of multicriteria decision analysis to geoelectric and geologic parameters for spatial prediction of groundwater resources potential and aquifer evaluation. *Journal of Pure and Applied Geophysics* 170:453–471. https://doi.org/10.1007/s00024-012-0501-9.

Adiat, K.A.N., Osifila, A.J., Akinlalu, A.A. and Alagbe, O.A. (2018). Mining of geophysical data to predict groundwater prospect in a basement complex terrain of southwestern Nigeria. *International Journal of Science and Technological Research* 7(5). ISSN 2277-8616.

Adiat, K.A.N., Ajayi, O.F., Akinlalu, A.A. and Tijani, I.B. (2020). Prediction of groundwater level in basement complex terrain using artificial neural network: a case of Ijebu–Ijesa, southwestern Nigeria. *Journal of Applied Water Science.* 10:8. https://doi.org/10.1007/s13201-019-1094-6.

Ajayi, C.A., Akintorinwa, O.J., Ademilua, O.L. and Adeoye, O.S. (2019). Relationship between magnetic susceptibility and gravity of basement rocks in southwestern Nigeria. *IOSR Journal of Applied Geology and Geophysics* 7(2):1. 46–57.

Akinlalu, A. A., Adegbuyiro, A., Adiat, K. A. N., Akeredolu, B. E. and Lateef, W. Y. (2017). "Application of multi-criteria decision analysis in prediction of groundwater resources potential: a case of Oke-Ana, Ilesa Area, Southwestern, Nigeria" NRIAG *Journal of Astronomy and Geophysics*, Vol 6, pp. 182–200.

Akinlalu, A.A. and Afolabi, D.O. (2018). Borehole depth determination to freshwater and well design using geophysical logs in coastal regions of Lagos, Southwestern Nigeria. Journal of *Applied Water Science* 8:152. 1–17. https://doi.org/10.1007/s13201-018-0798-3.

Akinlalu, A.A., Mogaji, K.A. and Adebodun, T.S. (2021). Assessment of aquifer vulnerability using a developed "GODL" method (modified GOD model) in a schist belt environ, southwestern Nigeria. *Journal of Environmental Monitoring and Assessment* 193:199. https://doi.org/10.1007/s10661-021-08960-z.

Alcamo, J. (2007). Future long-term changes in global water resources driven by socio economic and climatic changes. *Journal of Hydrological Science* 52 (2), 247–275.

Al-Abadi, A. M. and Shahid, S. (2015). A comparison between index of entropy and catastrophe theory methods for mapping groundwater potential in an arid region. *Journal of Environmental Monitoring and Assessment* 130:121.

Al-Abadi, A.M., Al-Shamma'a, A.M. and Aljabbari, M.H, (2016). A GIS-based DRASTIC model for assessing intrinsic groundwater vulnerability in northeastern Missan governorate, southern Iraq. *Journal of Applied Water Science* 7:89–101.

An, P., Moon, W.M. and Rencz, A.N. (1991). Application of fuzzy theory for integration of geological, geophysical and remotely sensed data. *Canadian Journal of Exploration Geophysics* 27, 1–11.

Anudu, G.K., Onuba, L.N. and Ufondu, L.S. (2011). Geoelectric sounding for groundwater exploration in the crystalline basement terrain around Onipe and adjoining areas, Southwestern Nigeria. *Journal of Applied Technology, Environment and Sanitation* 1 (4), 343–354.

Ayşegül, T.I. and Esra, A.A. (2017). The Decision-Making Approach Based on the Combination of Entropy and Rov Methods for the Apple Selection Problem. *European Journal of Interdisciplinary Studies* Volume 3, Issue 3.

Batayneh, A.T. (2010). Mapping Quaternary deposits in the El-Jufr playa (Southwestern Jordan plateau) using geoelectrical techniques: implications for geology and hydrogeology. *Journal of Science, Research and Essays* 5 (20), 3183–3192.

Bayode, S., Ojo, J.S. and Olorunfemi, M.O. (2007). Geoelectric characterization of aquifer types in the basement complex terrain of parts of Osun State, Nigeria. *Global Journal of Pure and Applied Sciences.* 12(3):377–385.

Bhattacharya, P.K, Patra, H.P. (1968). Direct Current Geoelectric, Sounding Methods in Geochemistry and Geophysics. *Elsevier*, Amsterdam, p. 135.

Bonham-Carter, G.F. (1994). Geographic Information Systems for Geoscientists: Modeling with GIS. Pergamon Press, Oxford, 398 p.

Carranza, E.J.M. (2008). Geochemical Anomaly and Mineral Prospectivity Mapping in GIS. Handbook of Exploration and Environmental Geochemistry, vol. 11. Elsevier, Amsterdam, p. 351.

Carranza, E.J.M. and Hale, M. (2002). Evidential belief functions for data-driven geologically constrained mapping of gold potential, Baguio district, Philippines. *Ore Geology Reviews 22*, 117–132.

Cheng, Q., Agterberg, F.P., and Ballantyne, S.B. (1994). The separation of geochemical anomalies from background by fractal methods. *Journal of Geochemical Exploration, 51*, 109–130.

Chowdhury, A., Jha, M.K., Chowdary, V.M. and Mal, B.C., (2009). Integrated remote sensing and GIS-based approach for assessing groundwater potential in West Medinipur district, West Bengal India. *International Journal of Remote Sensing*. 30 (1), 231–250.

Chung, C.F. and Moon, W.M. (1990). Combination rules of spatial geoscience data for mineral exploration. *Journal of Geoinformatics 2*, 159–169.

Corsini., A., Cervi, F. and Ronchetti, F. (2009). Weight of evidence and artificial neural networks for potential groundwater spring mapping: an application to the Mt. Modino area (Northern Apennines, Italy). *Journal of Geomorphology* 111:79–87.

Drobne, S. and Lisec, A. (2009). Multi–attribute decision analysis in GIS: weighted linear combination and ordered weighted averaging. *Informatica* 33: 459–474.

Environmental Systems Research Institute (ESRI). (2016). Inverse distance weighted interpolation.

Forson, A. Y. and Whiteman, D. (2014). Electrical resistivity charactarization of anisotropy in the Biscayne aquifer. *Groundwater* 52(5): 728-736.

Forson, E.D., Menyeh, A., Wemegah, D.D., Danuor, S.K., Adjovu, I. and Appiah, I. (2020). Mesothermal gold prospectivity mapping of the southern Kibi-Winneba belt of Ghana based on Fuzzy analytical hierarchy process, concentration area (C-A) fractal model and prediction-area (P-A) plot. *Journal of Applied Geophysics 174:* 1-12.

Jenifer, M.A. and Jha, M.K. (2017). Comparison of analytic hierarchy process, catastrophe and entropy techniques for evaluating groundwater prospect of hard–rock aquifer systems. *Journal of hydrology*. 1–16.

Knochenmus, L. A. and Robinson, J. L. (1996). Descriptions of anisotropy and heterogeneity and their effect on groundwater flow and areas of contribution to public supply wells in a karst carbonate aquifer system. USGS water-supply Report 47. Reston. Virginia: USGS.

Lashkaripour, G.R. (2003). An investigation of groundwater condition by geoelectric resistivity method: a case study in Korin aquifer, Southeast Iran. *Journal of Spatial Hydrol*ogy 3 (1), 1–5.

Lee, S. Kim, Y., Song Y. K. and Park, I., (2012). Regional groundwater productivity potential mapping using a geographic information system (GIS) based artificial neural network model. *Journal of Hydrology* 20, 1511-1527, doi: 10.1007/s10040-012-0894-7.

Lee, S, Kim, Y. S. and Oh, H.J. (2012). Application of a weights-of-evidence method and GIS to regional groundwater productivity potential mapping. *Journal of Environmental Management* 96(1):91–105.

Loke, M.H. (1999). Electrical imaging surveys for environmental and engineering studies. A practical guide to 2-D and 3-D surveys. *Terraplus Information*., pp. 67.

Madruccin, V., Taioli, F. and DeAranjo, C.C. (2008). Groundwater favourability map using GIS multicriteria data analysis on crystalline terrain, Sa Panlo State, Brazil. *Journal of Hydrology* 357(3–4): 153-173.

Mogaji, K.A., Lim, H.S. and Abdullah, K. (2015) Regional prediction of groundwater potential mapping in a multifaceted geology terrain using GIS-based Demspter-Shafer model. *Arabian Journal of Geosciences*. 8(5):3235–3258.

Moon, W.M. (1990). Integration of geophysical and geological data

using evidential belief function. *IEEE Transactions of Geoscience and Remote Sensing 28*, 711–720.

Nampak, H., Pradhan, B. and Manap, M.A. (2014). Application of GIS based data driven evidential belief function model to predict groundwater potential zonation. *Journal of Hydrology* 513:283–300.

Nykanen, V. and Salmirinne, H., (2007). Prospectivity for gold using regional geophysical and geochemical data from the Central Lapland Greenstone Belt, Finland. *Geological Survey of Finland Special Report 44*, 251–269.

Ojo, J.S., Olorunfemi, M.O. and Falebita, D.E. (2011) An Appraisal of the Geologic Structure beneath the Ikogosi Warm Spring in SouthWestern Nigeria Using Integrated Surface Geophysical Methods. *Earth Sciences Research Journal*. 15 (1): 27-34.

Olajide, A., Akinlalu, A.A. and Omosuyi, G.O. (2022). Application of GIS-Based Frequency Ratio Model to Geoelectric Parameters for Groundwater Potential Zonation in a Basement Complex Terrain. *Indonesian Journal of Earth Sciences*, Vol. 2, No. 1 (2022): 16-32. P-ISSN: 2798-1134 | E-ISSN: 2797-3549 | DOI: 10.52562/injoes.v2i1.295.

Ogundana, A.K. and Talabi, A.O. (2014). Groundwater Potential Evaluation of College of Engineering, Afe Babalola University, Ado-Ekiti, Southwestern Nigeria. *American Journal of Water Resources*, 2014, Vol. 2, No. 1, 25-30.

Oh, H.J., Kim, Y.S., Choi, J.K., Park, E. and Lee, S. (2011). GIS mapping of regional probabilistic groundwater potential in the area of Pohang City, Korea. *Jounral of Hydrology* 399:158–172. doi:10.1016/j.jhydrol.2010.12.027.

Oladunjoye, M.A., Korode, I.A. and Adefehinti, A. (2018). Geoelectrical exploration for groundwater in crystalline basement rocks of Gbongudu community, Ibadan, southwestern Nigeria. *Global Journal of Geological Sciences* 17: 25–43.

Olayinka, A.I. and Olorunfemi, M.O. (1992). Determination of Geoelectrical Characteristics in Okene Area and Implications for Borehole Siting. *Journal of Mining and Geosciences* 28(2). 403–412.

Olayinka, A.I., Abimbola, A.F., Isibor, R.A. and Rafiu, A.R., (1999). A geoelectrical hydrogeochemical investigation of shallow groundwater occurrence in Ibadan, southwestern Nigeria. *Journal of Environment and Geology* 37 (1–2), 31–39.

Olayinka, A.I. (1996). Non Uniqueness in the Interpretation of Bedrock Resistivity from Sounding Curves and its Hydrological Implications. *Journal of Water Resources*, 7(1&2): 55–60.

Olorunfemi, M.O. (1990). The hydrogeological implication of topographic variation with overburden thickness in Basement Complex Area of Southwestern Nigeria. *Journal of Mining and Geosciences* 26(1):1.

Olorunfemi, M.O. and Olarewaju, V.O, Alade, O. (1991). On the electrical anisotropy and groundwater yield

in a Basement Complex area of Southwestern Nigeria. *Journal of African Earth Sciences* 28(2):221–229.

Olorunfemi, M. O. and Okhue, E. T. (1992) Hydrogeological and Geologic significance of a geoelectric survey at Ile-Ife. Nigeria. *Journal of Mining and Geosciences*, 28, pp. 221–229.

Olorunfemi, M. O. and Ojo, J. S. and Akintunde, O. M. (1999). Hydrogeophysical evaluation of the Groundwater otential of Akure metropolis, southwestern Nigeria. *Journal of Mining and Geosciences* Vol. 25 (No. 2) PP. 207–228.

Omosuyi, G.O., Ojo, J.S. and Enikanselu, P.A. (2003). Geophysical investigation for groundwater around Obanla—Obakekere in Akure area within the Basement Complex of South-Western Nigeria. *Journal of Mining and Geosciences* 39(2):109–116.

Omosuyi, G.O. (2010). Geoelectric assessment of groundwater prospect an vulnerability of overburden aquifers at Idanre, Southwestern Nigeria. *Ozean Journal of Applied Sci*ences 3 (1), 19–28.

Omosuyi, G.O. and Oyemola, I.O. (2012). An assessment of hydrogeologic of characteristics of Bamikemo's hard rock terrain using geophysical techniques. *International Journal of Water Resources Environment and Engineering* 4:5. 120–133.

Omotoyinbo, O. S. (1994). Geology of Ado-Ekiti, (Unpublished thesis), Ondo State University Of Ado-Ekiti. Pp 84.

Oyawoye, M.O. (1961). On an occurrence of fayalite quartz-monzonite in the basement complex around Bauchi, Northern Nigeria. *Geological Magazine* 98(6):473-82

Oyawoye MO. (1965). Bauchite: a new variety in the quartz monzonitic series. *Nature.* 205(4972):689.

Ozdemir, A. (2011). Using a binary logistic regression method and GIS for evaluating and mapping the groundwater spring potential in the Sultan Mountains (Aksehir, Turkey)," *Journal of Hydrology*, vol. 405, no. 1-2, pp. 123–136.

Pourtaghi, Z. S. and Pourghasemi, H. R. (2014). GIS-based groundwater spring potential assessment and mapping in the Birjand township, Southern Khorasan Provine, Iran. *Journal of Hydrology*, 22, 643-662.

Porwal, A., Carranza, E.J.M. and Hale, M. (2003). Knowledge-driven and data-driven fuzzy models for predictive mineral potential mapping. *Natural Resources Research 12*, 1–25.

Prasad, R. K., Mondal, N. C., Banerjee, P., Nandakumar, M. V., and Singh, V. S. (2008). Deciphering potential groundwater zone in hard rock through the application of GIS. *Journal of Environment and Geology*, 55, 467-475, doi: 10.1007/ s00254-007-0992-3.

Rahmati, O. and Melesse, A.M. (2016). Application of Dempster–Shafer theory, spatial analysis and remote sensing for groundwater potentiality and nitrate pollution analysis in the semi-arid region of Khuzestan. *Iran Science of the Total Environment*. 568:1110–1128

https://doi.org/10.1016/j.scitotenv.2016.06.176.

Razandi, Y., Pourghasemi, H.R., Neisani, N.S. and Rahmati, O. (2015). Application of analytical hierarchy process, frequency ratio, and certainty factor models for groundwater potential mapping using GIS. *Journal of Earth Sciences Inf*ormation 8, 867–883.

Reilly, T., Dennehy, K.F., Alley, W.M., Cunningham, W.L. (2008). Groundwater availability in the United State. US Geological Society Circular 1323, 70p.

Ritzi, R. W. and Andolsek, R. H. (1992). Relation between anisotropic transmissivity and azimuthal resistivity surveys is shallow, fractured, carbonate flow systems. *Groundwater* 30(5): 774-780.

Shannon C. E. (1948). A mathematical theory of communications. *Journal of Bells Labs Technology*, 27(3), 379-423.

Shevyrev, S. and Carranza, E.J.M. (2022). Application of maximum entropy for mineral prospectivity mapping in heavily vegetated areas of greater Kurile Chain with Landsat 8 data. *Ore geology reviews.* 142: 1–15.

Srivastava, P.K. and Bhattacharya, A.K. (2007). Groundwater assessment through an integrated approach using remote sensing, GIS and resistivity techniques: a case study from a hard rock terrain. *International Journal of Remote Sensing* 27(20):4599–4620.

Watson, D.F. and Philip, G.M. (1985). A refinement of inverse distance weighted interpolation. *Geoprocessing* 2:315–327.

Webb, S.J., Ngobeni, D., Jones, M., Abive, T., Devkurran, N., Goba, R. and Ashwal, L.D., (2011). Hydrogeophysical investigation for groundwater at the Dayspring children's village, South Africa, *Leading Edge* 30(4), 434–440, doi:10.1190/1.

Xu, Y. Wu, Z. Long, J. and Song, X. (2014). A maximum entropy method for a robust portfolio problem. *Entropy, 16*, 3401–3415.

Yousefi, M. and Carranza, E.J.M. (2015). Geometric average of spatial evidence data layers: a GIS-based multi-criteria decision-making approach to mineral prospectivity mapping. *Journal of Computer and Geosciences 83:*72–79.